Heliyon 10 (2024) e40521

Contents lists available at ScienceDirect

Heliyon

journal homepage: www.cell.com/heliyon

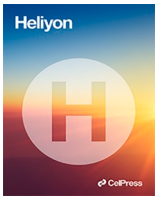

Research article

Exploring the dynamic world of ternary deep eutectic solvents: Synthesis, characterization, and key properties unveiled

Mshari A. Alotaibi [a], Tabassum Malik [b,**], A. Naeem [b], Amir Sada Khan [d], Israf Ud din [a,*], Maizatul S. Shaharun [c]

[a] Department of Chemistry, College of Science and Humanities, Prince Sattam bin Abdulaziz University, 16278, Al-Kharj, Saudi Arabia
[b] National Centre of Excellence in Physical Chemistry, University of Peshawar, Pakistan
[c] Department of Fundamental and Applied Sciences, Universiti Technologi PETRONAS, Malaysia
[d] Department of Chemistry, University of Science and Technology, Bannu, 28100, KPK, Pakistan

ARTICLE INFO

Keywords:
Ternary deep eutectic solvent
Ethaline
Glycine
Critical properties

ABSTRACT

Deep eutectic solvents are a novel class of solvents that have gained much attention with time due to their biodegradability, non-volatility, non-toxicity and low-cost. In this work, a novel ternary deep eutectic solvent (TDES) was synthesized using ethaline (ChCl:EG) and glycine, with the addition of carboxylic acids. The synthesized material was characterized through Fourier-transform infrared spectroscopy (FTIR). While the thermal stability and physical properties such as density, viscosity, surface tension and refractive index were also determined). To estimate the critical properties, modified version of Lyderson-Joback-Reid (LJR) and Lee-Kesler mixing (Alkhatib et al., 2020) [1] methods were used. The density of the DES was calculated using the Spencer and Danner correlation and the obtained values were compared with experimental data. FTIR analysis confirmed that hydrogen bonding is the main driving force responsible for the formation of the deep eutectic solvents. The physical properties of the binary DES system, such as viscosity, density,and thermal stability of the system were enhanced after the incorporation of a third component (carboxylic acid) to the system. However, the surface tension of the TDES system decrease with the increasing amounts of the third component, likely due to increase in the void radius of the TDES. Thus investigation is considering as novel work to check the influence of carboxylic acids on the physical properties of binary deep eutectic solvent systems.

1. Introduction

Ionic liquids (ILs) are designable organic electrolytes consisting of bulky organic cations and small organic or inorganic anions with melting points less than 100 °C due to organic cations. They can be easily designed by choosing the proper anion and cation. Originally organic cations have high melting points but after mixing them with inorganic anions they are converted into liquids having low melting points as compared to their precursor material. These low melting point mixtures are known as a eutectic mixtures. Ionic liquids have unique physical properties e.g., high boiling point, low vapor pressures under ambient conditions, odorless, and non-flammable nature making them attractive both academically as well as industrially [2–6]. Therefore, much of the interest in ILs

* Corresponding author.
** Corresponding author.
E-mail addresses: maliktabassum@uop.edu.pk (T. Malik), drisraf@yahoo.com (I. Ud din).

https://doi.org/10.1016/j.heliyon.2024.e40521
Received 18 October 2024; Accepted 18 November 2024
Available online 19 November 2024

has centered on the use of these deep eutectic solvent as alternatives to the volatile organic solvents. Due to these inherent properties, ILs are extensively used in various fields, such as material chemistry, biomass treatment, catalysis, and electrochemistry over the past 20 decades [7].

However, their synthesis requires a long reaction time and high-purity chemicals, even traces of impurity can affect its properties. Therefore, a large amount of salts is required for the formation of ILs to make complete exchange of ions completely, which makes the synthesis of ILs expensive [8]. This drawback limits the use of ILs as an industrial solvent. Nevertheless, to solve this issue, an emerging class of solvent that is deep eutectic solvents (DES) has been introduced having high biodegradability, low toxicity and cost-effective as compared to ionic liquids. The DES can be easily formed by mixing two environment-friendly components i.e. hydrogen bond donor (HBD) and acceptor (HBA), resulting in the formation of a eutectic mixture [9–11].

In this study carboxylic acid were added to the binary DES system to make the ternary deep eutectic solvent (TDES) [12–14] to work as catalyst and solvent system simultaneously to make the new approach for different types of applications to replace binary DES system such as in extraction, organic synthesis, biomass treatment, electrolyte in batteries etc. Sufficient data on TDES was obtained by measuring the physical properties (such as viscosity, density, surface tension, and refaractive index and FTIR and TGA analysis was done to confirm the formation and thermal stability (see Table 4)

2. Experimental

2.1. Chemicals and materials

Choline Chloride (ChCl, ≥98 %) was obtained from Sigma Aldrich and applied as received. Malonic acid synthetic grade ($CH_2(COOH)_2$, 99 %), oxalic acid ($C_2H_2O_4$) Tartaric acid reagent grade ($C_4H_6O_6$, 98 %) were purchased from Scharlau. Ethylene glycol analytical reagent ($(CH_2OH)_2$, ≥99.08 %) was purchased from BDH Lab suppliers.

2.2. Instrument employed

Characterization of deep eutectic solvent was performed using FTIR (1000 PerkinElmer) analysis for functional group elucidation in the range of 500-4000 cm^{-1}. The viscosity of synthesized TDES was measured using QCM (quartz crystal microbalance) and density via specific gravity bottle at room temperature (25 °C). While the refractive index and surface tension of the samples was measured using Bellingamn/Stanley RFM732 Refractometer and Tensiometer K9 model K9MK1 respectively. Moreover, thermal stability was determined using TGA (Mettler Toledo TGA/SDTA85/e).

2.3. Synthesis of deep eutectic solvent

In the present work, deep eutectic solvents (DESs) were synthesized by a simple mixing method [15,16]. The precursors were first dried for 3hrs at 80 °C in a vacuum oven to remove the moisture contents. An optimized molar ratio of 1:4 of choline chloride (ChCl) and ethylene glycol/Glycerol was mixed and heated at 80 °C in an oil bath at 500 rpm until the formation of transparent homogenous liquid. The mixture was allowed to cool at room temperature. After that, the synthesized DES was kept overnight to ensure that no precipitation occurs. From these binary DES, ternary DES (TDES) was synthesized by adding different molar ratios of one of three carboxylic acid into it and heated in an oil bath at 80 °C at a stirring rate of 500 rpm until the formation of a homogenous liquid (Table 1). Only those TDES were selected for further study that exhibit long-term stability and remained liquids at room temperature without converting into semi-solid crystals or precipitate formation after cooling at room temperature. Subsequently, the DES was cooled and stored in a desiccator before characterization and to be used as a solvent. In Fig. 1, all synthesized TDES system are shown.

To use the deep eutectic solvents in any desired application, it is necessary to measure their physical properties (density, surface tension, viscosity, and refractive index) and thermal stability. Moreover, thermodynamic models were also applied to validate the experimental data to measure the critical properties of the material.

Thus, in this study physiochemical properties, thermal stability and critical properties including critical temperature (T_c), critical volume (V_c), critical pressure (P_c), normal boiling point (T_b) and acentric factor (ω) of the synthesized TDES were measured and compared with the binary DES system.

Table 1
Composition and abbreviations of studied TDES.

Salt (HBA)	HBD_1	HBD_2	Molar ratio	Abbreviations
Choline Chloride (ChCl)	Ethylene Glycol (EG)	Malonic Acid (MA)	1:4: (1–11)	CEM
		Oxalic Acid (OA)	1:4: (1–4)	CEO
		Tartaric Acid (TA)	1:4: (1–6)	CET
	Glycerol (G)	Malonic Acid (MA)	1:4: (1–11)	CGM
		Oxalic Acid (OA)	1:4: (1–4)	CGO
		Tartaric Acid (TA)	1:4: (1–6)	CGT

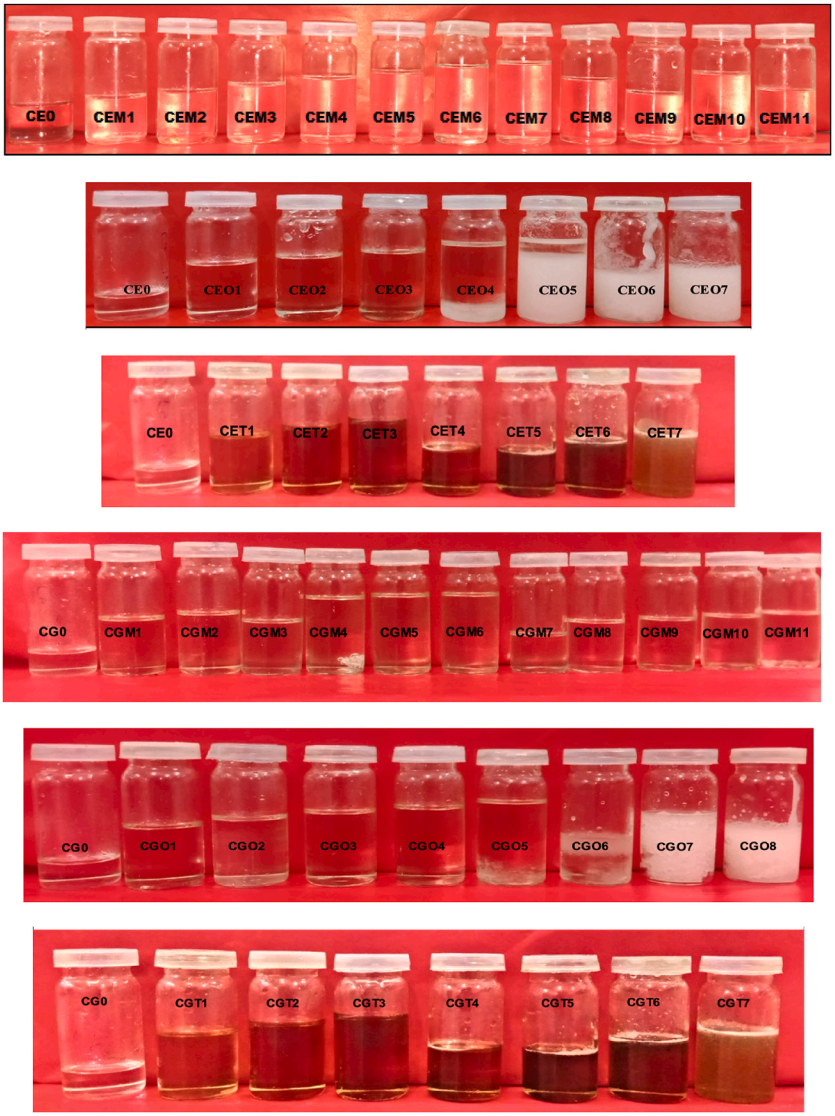

Fig. 1. Carboxylic acid based Ethaline and Glyceline TDES.

3. Results and discussion

3.1. Physical properties

The physical properties of all synthesized deep eutectic solvents were determined at room temperature 25 °C.

3.1.1. Viscosity

Viscosity plays an important role in the removal process as easy mass transfer is required for the liquid-liquid extraction process. Table 2shows that the viscosity of all TDES increases with the increase in the molar ratio of the hydrogen bond donor. This increase may be due to the increasing number of hydrogen bonds which makes the solvent more viscous [7]. The viscosity of the systems can also be observed physically that with the increasing concentration of hydrogen bond donor, they appear like honey. Furthermore, it can also be seen from Table 2 that the viscosity was also increases with the increase in void radius, as reported by many researchers [17]. It can be seen clearly that the system with more OH shows maximum viscosity due to the possibility of the formation of more numbers of hydrogen bonds such as in the case of using tartaric acid [17] (see Table 3).

3.1.2. Density

Density is one of the important parameters to understand the physical behavior of any solvent. Table 2 shows the density of most deep eutectic solvents lies between 1.01 g/cm^3 and 1.6 g/cm^3 as reported [18]. Similar results were also observed from current

Table 2
Physical properties of deep eutectic solvents.

DES	Density	Viscosity (cp)	Surface tension (mN/m)	Void Radius (Å)	Refractive Index
CE	1.0101 ± 0.02	218 ± 2	43 ± 0.62	1.632 ± 0.011	1.57 ± 0.54
CEM1	1.0112 ± 0.04	225 ± 4	41 ± 0.408	1.661 ± 0.008	1.57 ± 0.46
CEM5	1.0179 ± 0.03	241 ± 3	38 ± 0.43	1.732 ± 0.007	1.56 ± 0.43
CEM10	1.1249 ± 0.01	254 ± 1	37 ± 0.57	1.774 ± 0.013	1.57 ± 0.54
CEO1	1.012 ± 0.05	225 ± 3	39.8 ± 0.36	1.69 ± 0.0076	1.56 ± 0.34
CEO4	1.0144 ± 0.04	241 ± 5	38.5 ± 0.44	1.72 ± 0.0101	1.54 ± 0.75
CET1	1.1125 ± 0.03	248 ± 3	54 ± 0.77	1.46 ± 0.01	1.59 ± 0.7
CET3	1.1359 ± 0.05	354 ± 5	37.3 ± 1.5	1.75 ± 0.03	1.54 ± 0.12
CET4	1.1432 ± 0.02	418 ± 4	–	–	1.53 ± 0.43
CG	1.01 ± 0.01	215 ± 3	40 ± 1	1.69 ± 0.017	1.60 ± 0.65
CGM1	1.0131 ± 0.04	220 ± 5	38.03 ± 0.57	1.73 ± 0.011	1.59 ± 0.6
CGM4	1.0159 ± 0.06	230 ± 4	34.77 ± 0.416	1.81 ± 0.009	1.58 ± 0.75
CGM10	1.0146 ± 0.02	248 ± 4	29.5 ± 1.4	1.972 ± 0.039	1.576 ± 0.54
CGO1	1.0123 ± 0.01	226 ± 3	41.6 ± 2	1.66 ± 0.032	1.59 ± 0.85
CGO4	1.014 ± 0.04	245 ± 5	36.2 ± 0.58	1.77 ± 0.014	1.58 ± 0.45
CGT1	1.1201 ± 0.05	359 ± 5	40.3 ± 0.35	1.68 ± 0.006	1.60 ± 0.54
CGT2	1.1234 ± 0.05	398 ± 3	38.83 ± 1.5	1.718 ± 0.028	1.54 ± 0.76
CGT4	1.1579 ± 0.04	509 ± 4	—[a]	—[a]	1.478 ± 0.5

[a] Solution was so viscous due to which surface tension was difficult to measure.

Table 3
FTIR peaks of ChCl:EG:M TDES.

Functional Groups	Frequency (cm^{-1})	Mode of vibrations
N-H	2869	Stretching
Cl	408 and 600	–
O-H	3200–3500	Stretching
C-H	2800–3000	Stretching
C-O	1695	Stretching

Table 4
FTIR peaks of ChCl:EG:Ox TDES.

Functional Groups	Frequency (cm^{-1})	Mode of vibrations
C-H	2947	Stretching
Cl	408 and 600	–
O-H	3700–3100	stretching Vibrations
O-H	3550 and 3230	Stretching
CH_2	1500 and 1100	Bending Vibrations
CH_2	884	Rocking
CH_2	1320 and 1300	Wagging
CH_2	1300 and 1200	Twisting
CH_2	1660–1610	Stretching
C-H	2800–3000	Stretching
C-O	1695	Stretching
C-C	875–840	Stretching

experimental data (Table 2). Density was determined using a simple method using the formula illustrated in eq. (3).

$$density\ (\rho) = \frac{mass(g)}{volume(mL)} \tag{1}$$

It was observed that the density of hydrophilic DES increased with increasing the concentration of carboxylic acid. The calculated value of the density was found to be greater than water, making hydrophilic DES denser as compared to water. Thus, phase separation from the non polar solvent system become easier due to the high desnity difference.

3.1.3. Surface tension

The surface tension is the measurement of intermolecular forces present in the solvent and is indicator to measure the energy required to form the void for the fitting of solute molecule in the solvent. Liquids with lower void energy are considered better for dissolving the solute molecule. From the surface tension, the void radius of the liquid can be calculated using Eq. (3),

$$4\pi < r^2 >= \frac{3.5KT}{\gamma} \tag{2}$$

By simplifying,

$$< r > = \sqrt{\left(\frac{3.5KT}{\Upsilon} x \frac{1}{\pi}\right)} \quad (3)$$

where k is Boltzmann's constant, T is the absolute temperature and ϒ is the surface tension of DES at room temperature. From the equation, it can be seen there is an inverse relationship between the void radius and the square root of the surface tension [19].

As can be seen from Table 2, that with the decrease in surface tension the void radius of the solvent increased and less energy was required for the solute molecule to fit into the void or to interact with the solvent.

3.1.4. Refractive index

The speed of light in the solution varies within the solvent depending on the homogeneity of the solvent. The presence of sample particles in the mixture reflects, refract, and scatters the light, causing it to refracts at different angles. From the literature, it was found that the refractive index of most binary DES systems lies within the range of 1.48–1.6 nD [20]. To study the influence of the carboxylic group the refractive index of the selected DES was measured. It was obtained in the range of 1.4–1.7, which is comparable to the results reported in the literature. It can be observed that no significant change in the refractive index was noted, as no suspended particles were detected in any of the cases, and a homogenous mixture was observed. Another reason for the lack of significant change is that no prominent variation in density was observed, as the refractive index typically depends on the density, thus, all TDES systems have almost the same refractive index.

3.2. FTIR analysis of TDES system

3.2.1. FTIR analysis of Ethaline:Malonic acid

The FT-IR spectra in Fig. 2 relate the FT-IR spectra of ethaline and ethaline: malonic acid. The appearance of broad peak near 1696 cm^{-1} represented the stretching band of carbonyl group (-CO) in the malonic acid. The OH stretching spectrum in the IR confirms the interaction of $Cl^{-}$of choline chloride with the -OH groups of ethylene glycol and malonic acid through hydrogen bonding. The formation of hydrogen bonding is further confirmed by the stretching region of the OH group in the FT-IR spectrum. Moreover, strong broad overlapping peaks centered below 3100 cm^{-1} were observed in the spectrum of malonic acid, attributed to the strong hydrogen-bonding of dimer rings present in carboxylic acids. However, the peak at 3100 cm^{-1} became sharper and exhibited overlap due to liquid formation. A new broad peak appeared of at 3332 cm^{-1} in the FT-IR spectrum of the ethaline:malonic acid TDES confirming the presence of hydroxyl groups of malonic acid and ethylene glycol, relates to the weak hydrogen bond formation [21]. Thus the presence of a broad peak of hydroxyl group in the stretching region of IR indicated the presence of a number of hydrogen bonds between OH group of choline, and OH group of malonic acid and ethylene glycol. As a result of the formation of these hydrogen bonds, the lattice energy of the molecule of choline chloride decreased that results in the formation of the deep eutectic solvent having a low melting point as compared to the original component. The deep eutectic solvents formed is colorless, and transparent liquid at room temperature due to the vast hydrogen bonding network.

3.2.2. FTIR analysis of Ethaline:Oxalic acid

Fig. 3 shows the FT-IR spectra of pure oxalic acid, choline chloride, ethylene glycol and oxalic acid-based TDES. The peak appeared at 1660 cm^{-1} corresponds to the deformation band shifting of OH group, which confirmed the formation of the H-bond in the deep

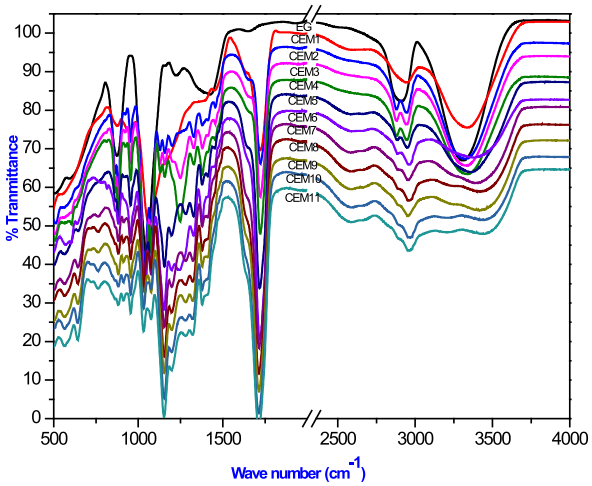

Fig. 2. FTIR spectra of ethaline: malonic acid DES with varying concentration of malonic acid.

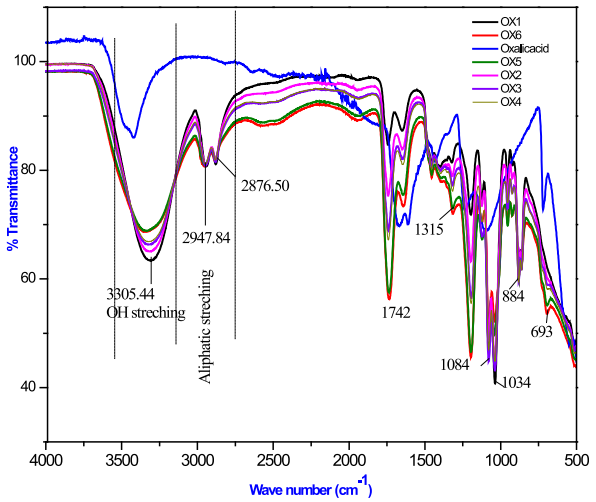

Fig. 3. FTIR spectra of ethaline: oxalic acid TDES with varying concentrations of oxalic acid.

eutectic solvent.

The stretching hydroxyl vibrational peak of choline chloride shifts to the lower wavenumber confirming the interaction of OH of oxalic acid with the Cl ion of choline chloride. The broad band in the range of 3100–3700 cm^{-1} confirms the presence of OH stretching vibrations, which widen with the increase in the concentration of oxalic acid confirming the increase in the number of hydrogen bonds. The OH stretching bands in the water, alcohol and phenols range between 3400 and 3800 cm^{-1}, as no peak is observed in this region thus confirming that low water content was present in DES. The peak in the range of 1100–1500 cm^{-1} is assigned to CH_2 bending vibrations, while the peak appeared at 884 cm^{-1} was assigned to rocking vibrations of CH_2 group. The CH_2 wagging at appeared at 1320 and 1300 cm^{-1}, the CH_2 twisting at 1300 and 1200 cm^{-1} were observed in the spectra of all TDESs. The peak appeared at 1660–1610 is usually assigned to stretching vibrations of CH = CH_2 [22–24]. Aissaoui et al. reported similar investigation for MTPPB-EG DES system [21]. The peak observed in the range of 1410-1400 cm^{-1} is assigned to bending vibration of C-OH. This peak was investigated in the spectra of all TDESs. The peak appeared in the range of 875-840 cm^{-1} is assigned to stretching vibrations of C-C group.

3.2.3. *FTIR analysis of Ethaline:Tartaric acid*

Fig. 4 showed the FTIR spectra of ChCl:EG with varying compositions of tartaric acid. The FTIR spectra of all deep eutectic solvent show a broad peak in the range of 3150-3450 cm^{-1} which corresponds to the OH stretching vibration. This peak broadens with the increasing concentration of tartaric acid, confirming the formation of intermolecular hydrogen bonding. The characteristic peak at 1722 cm^{-1} is attributed to the -C=O stretching vibrational peak which is absent in the case of Ethaline DES, and sharpens with the increase in the concentration of tartaric acid. The appearance of broad peak at 2907 cm^{-1} confirmed the presence of hydrogen bonds

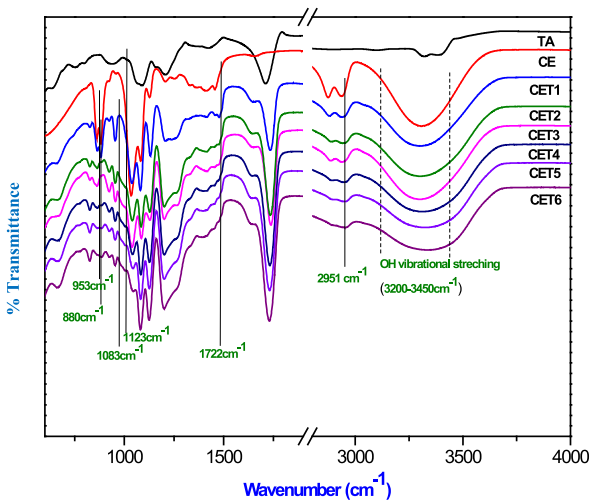

Fig. 4. FTIR spectra of ethaline: tartaric acid DES with varying concentrations of tartaric acid.

that widen with the increasing concentration of tartaric acid, due to the increased number of hydrogen bonds. Thus, hydrogen bonding results in the increase in the length of the OH bond and reduces its stretching frequency. The peak at 2951 cm^{-1} was assigned to -CH_2- antisymmetric vibrational stretching. The sharp and strong peak observed at 1123 cm^{-1} corresponds to the stretching vibrations of -C-H bond. The presence of peaks in the range of 900 cm^{-1} to 1000 cm^{-1} indicated the presence of quaternary ammonium compounds. The peak at 953 cm^{-1} was attributed to the C- N group of ChCl [25].

3.2.4. FTIR analysis of Glyceline:Malonic acid

In order to study the H-bonding strength between ChCl, glycerol and malonic acid FTIR analysis was done in the range of 500–4000 cm^{-1} as shown in Fig. 5. The FTIR spectra showed the H-bond interaction between choline chloride and glycerol and the effect of malonic acid concentration on H-bond strength present in glyceline. The peak observed in the range of 3200–3400 cm^{-1} was attributed to the OH stretching vibration after the formation of glyceline. While in the case of glycerol stretching peak was observed at 3320-3345 cm^{-1} [26]. A Strong, broad overlapping peaks was observed below 3270 cm^{-1} after the addition of malonic acid, which broadened with the increase in the concentration of malonic acid, which is due to the formation of strong hydrogen bonds due to presence of dimer rings in malonic acid. A strong broad peak observed at 1695 cm^{-1} responds to the carbonyl stretching (C=O) region of malonic acid [27] Nevertheless, after the addition of malonic acid, this peak shifted toward a higher wavenumber and was observed at 1730 cm^{-1}. Two free free groups are present in carboxylic acid i.e. -OH and -C=O in gaseous or extremely dilute solution. Perkin et al. [28] provided the computational and experimental evidence of the above work in detail. Thus, in the eutectic mixture the -C=O group of malonic acid is free while OH- group is bonded to the Cl-of the choline chloride and showed the shift of wavenumber. The broadband was observed in the 3200-3450 cm^{-1} which got wider with the increase of concentration of malonic acid revealing the presence of various hydrogen bonds inside the molecule.

3.2.5. FTIR analysis of Glyceline:Oxalic acid

FTIR analysis of glyceline and glyceline: oxalic acid with varying concentrations of oxalic acid is shown in Fig. 6. The peak at 1737 cm^{-1} indicates the presence of free -C=O group of oxalic acid which sharpened with the increase of concentration of oxalic acid. After adding the glycerol broad stretching peak was observed at 3320-3345 cm^{-1} [26]. The peak at 1030 cm^{-1} was attributed to the -OH deformation band. Certain peaks were observed after formation of DES at 1737 cm^{-1}, 1457 cm^{-1}, 1205 cm^{-1}, 1305 cm^{-1}, 1039 cm^{-1} and 951 cm^{-1} indicated N-H bending, H-bending, CH_2 deformation, -CH bending, C-C stretching and N-C-C bending vibrations respectively. The peak of oxalic acid at 1630 cm^{-1} and 1207 cm^{-1} became stronger after increasing the concentration of oxalic acid. While, CGM having a sharp peak at 1730 cm^{-1} indicates the presence of a bonded and free carbonyl group. The effect of an increase in the molar ratio of oxalic acid can be easily seen from the spectra (Fig. 6). With further increase the concentration of oxalic acid, the interaction of HBD-HBD in disproportion weakens the H-bonding between the molecules resulting in semi-solid substance. These results suggest that several types of H-bond may be present in TDES, i.e. Ox (OH)—Cl (ChCl), Ox (OH)-Ox(OH), Gly-Gly, ChCl (OH)-Cl, Gly-Ox and Gly(OH)- (Cl) ChCl.

3.2.6. FTIR analysis of Glyceline:Tartaric acid

As mentioned in the earlier sections, a broad band in the range of 3320–3345 cm^{-1} was assigned to the OH stretching vibrations (Fig. 7). The sharp peak at 1730 cm^{-1} was detected after the addition of tartaric acid and sharpened more with an increasing concentration of tartaric acid. The corresponding peak indicates the presence of unbounded carbonyl groups (-C=O), which were not present in the case of CG system, confirming the presence of tartaric in newly synthesized TDES [25]. Further, the peak at 2935 cm^{-1} was assigned to the -CH_2- groups as discussed in previous cases. The peak for choline chloride was detected in the range of 900 cm^{-1} to 1000 cm^{-1}.

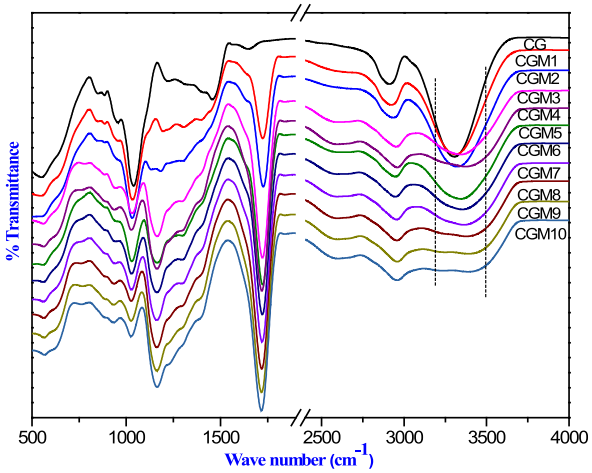

Fig. 5. FTIR spectra of Glyceline and Glyceline: malonic acid DES with varying concentration of malonic acid.

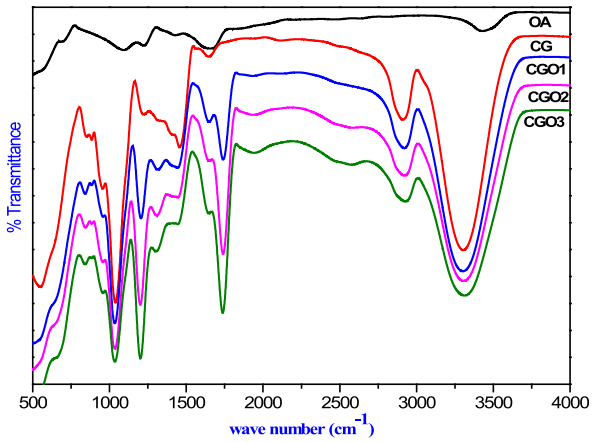

Fig. 6. FTIR spectra of Glyceline and Glyceline: malonic acid DES with varying concentrations of malonic acid.

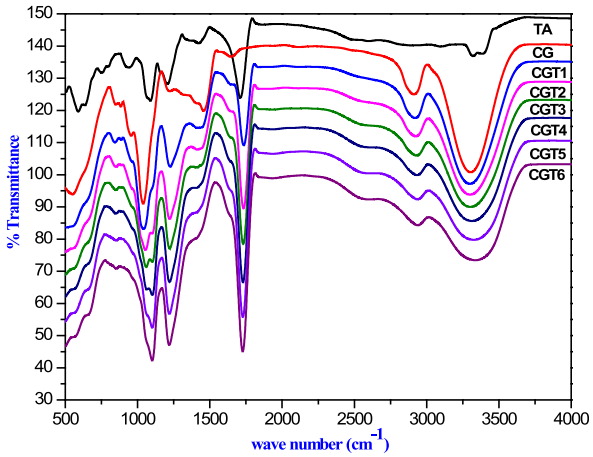

Fig. 7. FTIR spectra of CGT DES system with different concentrations of tartaric acid.

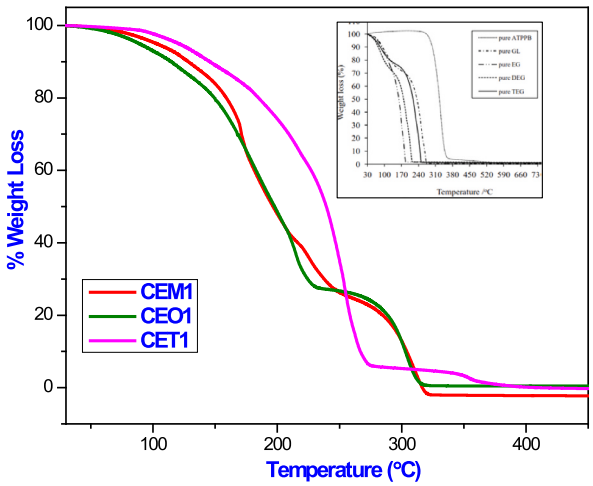

Fig. 8. TGA graph of malonic acid, oxalic acid and tartaric based ethaline.

3.3. Thermal stability of TDES system

3.3.1. TGA analysis of Ethaline:MA/OA/TA

Fig. 8 shows the comparison between the TGA curve of pure ethaline and oxalic, malonic and tartaric acid-based Ethaline DES. The weight loss together with the DTGA, indicates the stepwise decomposition. It can be seen from the graph that thermal decomposition for all three systems lies after 305 °C, which indicates the thermal stability of carboxylic acid-based ethaline. It was noted that the carboxylic acid-based ethaline was more stable as compared to the pure ethaline system [29]. Additionally, in comparison to ethaline, stepwise weight loss was observed in carboxylic based DES system. In comparison between the above three systems, the oxalic acid based DES showed more stability as compared to malonic and tartaric acid based Ethaline. In comparing the three systems, the decomposition temperature followed the trend, oxalic acid ≈ Malonic acid > tartaric acid, which is similar to the one observed for the DES system, CEO > CEM > CET [30].

3.3.2. TGA analysis of Glyceline:MA/OA/TA

Fig. 9 showed the TGA spectra of pure glyceline and carboxylic acid based Glyceline DES system. As can be seen from Fig. 9, the thermal stability of the binary DES was enhanced after adding the carboxylic acid to the glyceline system. Also, stepwise degradation was recorded in the case of carboxylic acid based glyceline. From the graph it can be seen initially that the water content has been removed up to 100 °C and after that the thermal degradation take place up to 300 °C with a gradual weight loss [31]. From Fig. 9, it is evident that as the temperature increases, the components of the system begin to decompose. Since hydrogen bonding is the primary force responsible for formation of the DES, its disruption due to decomposition or evaporation breaks the eutectic interactions that hold the system together. Here's the corrected version:

Fig. 9 shows that DES decomposes in two stages. The first step involves the evaporation of water and other volatile components, occurring between 110 °C and 150 °C. In the second step, from 150 °C to 300 °C, the degradation of the DES components takes place. In contrast, tartaric acid exhibits single-step degradation between 100 °C and 300 °C, likely due to the higher number of hydroxyl groups, which may participate in hydrogen bonding. In comparison between carboxylic acid groups, a similar trend was noted as described in section 3.3.1. Different researchers reported that viscosity is directly proportional to the thermal stability of liquids. As we know that the viscosity of glycerol (1400 mPa s) was found to be higher in value as compared to ethylene glycol (16.617 mPa s). As such, the thermal stability of carboxylic acid based glyceline is greater than carboxylic acid based ethaline [30].

3.4. Estimation of critical properties

Critical properties of organic compounds were calculated using Lydersen-Joback-Reid method [32,33]. The proposed equations (4)–(7) were used for the calculation of Normal boiling temperature (T_b), Critical Volume (V_c), critical temperature (T_c) and Critical Pressure (P_c), of the organic molecules.

$$T_b = 198.2 + \sum n_i \Delta T_{bMi} \tag{4}$$

$$T_c = \frac{T_b}{0.5703 + 1.0121 \sum n_i \Delta T_{Mi} - \left(\sum n_i \Delta T_{Mi}\right)^2} \tag{5}$$

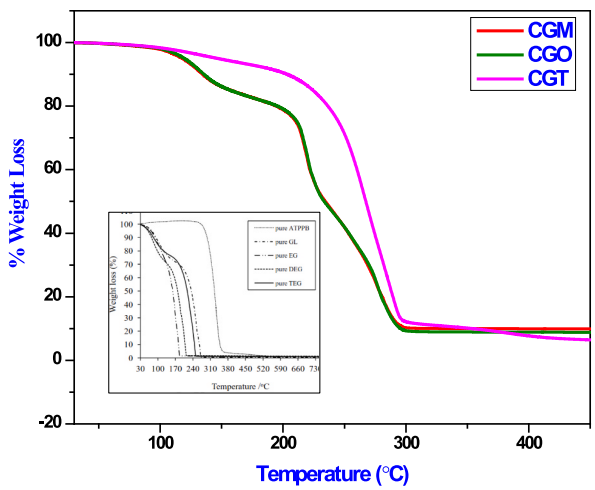

Fig. 9. TGA graph of malonic acid, oxalic acid and tartaric acid based Glyceline.

$$P_c = \frac{M}{(0.2573 + \sum n_i \Delta P_{Mi})^2} \tag{6}$$

$$V_c = 6.75 + \sum n_i \Delta V_{Mi} \tag{7}$$

whereas, n_i is the frequency of the number of ith group appear in the molecule,
$\Delta T_{Mi}\ (K)$ is the group contribution of ith group to the critical temperature of the molecule
$\Delta T_{bM}\ (K)$ is the group contribution of ith group to normal boiling temperature of the molecule
$\Delta V_{Mi}\ (cm^3/moL)$ is the group contribution of ith group to the critical volume of the molecule
$\Delta P_{Mi}\ (bar)$ is the group contribution of ith group to critical pressure of the molecule and
$M\ (g/moL)$ is the molecular weight of the molecule (see Table 5).

The groups involved in our study with their group contribution values are listed in Table 6. Thus, these equations are used to calculate the critical properties of individual molecules. As Deep eutectic solvent is the combination of two or more precursors so different methods were used for measuring the critical properties of the deep eutectic solvent. Researchers [1] recommended the Lee-Kessler [34] rule to estimate the critical properties of the deep eutectic solvents. The equations used to calculate the final critical properties include,

$$\boldsymbol{T_{cD}} = \frac{\mathbf{1}}{\boldsymbol{V_{cD}}^{0.25}} \sum_i \sum_j \sum_k \boldsymbol{y_i y_j y_k V_{cijk}}^{0.25} \boldsymbol{T_{cijk}} \tag{8}$$

Where,

$$T_{cijk} = \left(T_{ci} T_{cj} T_{ck}\right)^{0.5} k'_{ijk} \tag{9}$$

$$\boldsymbol{V_{cD}} = \sum_i \sum_j \sum_k \boldsymbol{y_i y_j y_k}\ \boldsymbol{V_{cijk}} \tag{10}$$

Where,

$$V_{cijk} = \frac{1}{8}\left(V_{ci}^{1/3} + V_{cj}^{1/3} + V_{ck}^{1/3}\right) \tag{11}$$

And,

$$P_{cD} = (0.2905 - 0.085\omega_D)\frac{RT_{cD}}{V_{cD}} \tag{12}$$

Where,

$$\omega_D = \sum_i y_i \omega_i \tag{13}$$

whereas, i, j and k refer to the pure components, y_i, y_j, and y_k refers to the mole fraction of the precursors used for the synthesis of deep eutectic solvent, D indicates the final properties of the mixture. P_{cD}, V_{cD}, T_{cD} and ω are critical pressure, critical volume, critical temperature, and acentric factor in bar, cm3/moL and K respectively for the ternary deep eutectic solvent mixture. Valderrama [35] proposed the equation for calculating the acentric factor of the precursor,

$$\omega = \frac{(T_b - 43K)(T_c - 43K)}{(T_c - T_b)(0.7T_c - 43K)} \log\left(\frac{P_c}{P_b}\right) - \frac{(T_c - 43K)}{(T_c - T_b)} \log\left(\frac{P_c}{P_b}\right) + \log\left(\frac{P_c}{P_b}\right) - 1 \tag{14}$$

whereas the equation used for the calculation of density from critical properties was proposed by Spencer and Danner [36]. The equation describes as follows,

$$\rho_L = \frac{MP_{cD}}{RT_{cD}}\left(\frac{0.3445 P_{cD} V_{cD}^{1,0135}}{T_{cD}}\right)^{\beta} \tag{15}$$

Where,

$$\beta = -\left[\frac{1 + (1 - T_R)^{2/7}}{1 + (1 - T_{bR})^{2/7}}\right] \tag{16}$$

$$T_R = \frac{T}{T_c} \tag{17}$$

And,

Table 5
FTIR peaks of ChCl:EG:TA TDES.

Functional Groups	Frequency (cm^{-1})	Mode of vibrations
C-N	953	
-CH_2-	2951	Vibrational streching
O-H	3150–3450	stretching
O-H	2907	
C-H	1123	Stretching
C=O	1722 cm^{-1}	Stretching vibrational

Table 6
Groups of atoms used in this work and their contribution to critical properties for the modified LJR method.

Group	ΔT_{bM}	ΔT_M	ΔP_M	ΔV_M
	K	K	Bar	cm^3/moL
-CH_3	23.58	0.028	0.3031	66.81
-CH_2-	22.88	0.016	0.0159	57.11
-CH<	21.74	0.0002	0.114	45.7
-OH (Alcohol)	92.88	0.072	0.0723	30.4
>N-	11.74	0.03	0.0304	26.7
-Cl	38.13	0.374	0.3738	62.08
-COOH	169.06	0.085	0.4537	88.6

$$T_{bR} = \frac{T_b}{T_c} \tag{18}$$

whereas, ρ_L (g/cm^3) is the estimated density of the ternary DES mixture, *M (g/moL)* is the molecular mass of the eutectic mixture. R is the universal gas constant with the value of 8.314J/moL/K. T_{cD} is the critical temperature (K) of the eutectic mixture, T_R and T_{bR} is the reduced temperature and reduced boiling point temperature, respectively. Thus, in this binary interaction parameter was considered as unity as reported by Nouman et al. [37]. Whereas, the deviation in density value of deep eutectic solvent calculated experimentally with the estimated values were calculated using the formula [37],

$$\%\Delta\rho = \frac{\rho_L - \rho_{exp}}{\rho_{exp}} X\,100 \tag{19}$$

whereas, %Δρ refers to the deviation of the value of density calculated experimentally to the estimated values. ρ_L and ρ_{exp} refers to the density values calculated using spencer and danner correlation and calculated experimentally, respectively.

In this work, an attempt has been made to classify the data on the based on the type of carboxylic acid added to the binary deep eutectic solvents (DES) and to study their effect on the different parameters. It can be seen from Table 7 that as with the increase in the concentration of carboxylic acid, the density of the system is increased in both estimated and experimental values but the deviation is observed. Thus with an increase of mass, deviation of experimental values from estimated values are noted. As incase of increasing ethaline very small deviation of 0.2 % was recorded, while after adding the malonic acid the positive deviation was noted which increase from 0.8 % to 23 %, this may be attribute to the estimation that more functional group provide greater availability of potential active sites for bonding. However, due to limited hydrogen bond acceptors (HBAs), not all active sites participate in bonding. Another reason may be that, due to the increased number of functional groups, the number of hydrogen bonds increases, but the strength of these bonds decreases, which may result in lower density values compared to the estimated ones [37].

Similar investigations were observed incase of adding oxalic acid to ethaline, and malonic acid and oxalic acid to Glyceline. However, an exception was observed incase of adding tartaric acid to ethaline and glyceline binary DES system in small amount. The negative deviation was observed with adding small amount of tartaric acid to ethaline and glyceline system which goes to positive with further increase in concentration. The deviation was observed from −6% to 8 % and −3%–8 % for ethaline and glyceline system after addition of tartaric acid, respectively. This may be due to availability of -OH functional group apart from carboxylic group in comparison with oxalic acid and malonic acid [37]. This effect may be due to the reason that -OH group also undergoes intramolecular hydrogen bonding which increase their density but with increase in further concentration causes the stearic hindrance for molecule to undergo intramolecular hydrogen bonding.

In the literature the deep eutectic solvents are considered as analogous to ionic liquid and according to the literature for the fixed value of 0.60 for T_b/T_c was assumed for ionic liquids to measure the normal boiling point temperature and critical temperature of ionic liquids but in case of deep eutectic solvents the value varies. So in this work values varies between 0.75 and 0.79 and it cannot be assumed that there is any fixed value of T_b/T_c. (Table 7).

Table 7
Estimated critical properties, viscosity and comparison of densities (at 25 °C) with experimental values for TDES.

DES	T_b (K)	T_c (K)	P_c [15]	V_c (cm^3/moL)	Z	ω	T_b/T_c	ρ_{est} (g/cm^3)	ρ_{exp} (g/cm^3)	Δρ (%)
$(ChCl:EG)_{1:4}$	435.26	568.61	54.32	233.53	0.268	1.35	0.765	0.96	1	0.2
$(ChCl:EG:MA)_{1:4:0.5}$	446.36	585.93	54.56	233.69	0.261	1.31	0.761	1.019	1.0112	0.819
$(ChCl:EG:MA)1_{:4:1}$	455.92	600.40	54.54	234.78	0.256	1.28	0.760	1.068	1.0118	5.563
$(ChCl:EG:MA)_{1:4:1.5}$	463.86	612.83	54.61	235.27	0.252	1.25	0.757	1.111	1.0126	9.689
$(ChCl:EG:MA)_{1:4:2}$	470.68	623.58	54.65	235.68	0.248	1.23	0.755	1.148	1.0154	13.068
$(ChCl:EG:MA)_{1:4:3}$	481.74	641.23	54.70	236.35	0.242	1.19	0.751	1.211	1.0179	18.935
$(ChCl:EG:MA)_{1:4:4}$	490.35	655.12	54.73	236.88	0.238	1.16	0.748	1.261	1.0197	23.641
$(ChCl:EG:MA)_{1:4:5}$	497.23	666.35	54.738	237.30	0.234	1.14	0.746	1.302	1.1131	16.960
$(ChCl:EG:MA)_{1:4:6}$	502.87	675.6	54.742	237.64	0.231	1.12	0.744	1.336	1.1138	19.967
$(ChCl:EG:MA)_{1:4:7}$	507.56	683.37	54.741	237.92	0.229	1.10	0.743	1.365	1.1242	21.441
$(ChCl:EG:MA)_{1:4:8}$	511.53	689.97	54.738	238.16	0.227	1.09	0.741	1.390	1.1249	23.581
$(ChCl:EG:MA)_{1:4:9}$	514.94	695.66	54.734	238.37	0.225	1.08	0.740	1.412	1.1388	23.973
$(ChCl:EG:OA)_{1:4:0.5}$	444.30	583.79	55.47	228.552	0.261	1.31	0.761	1.026	1.012	1.371
$(ChCl:EG:OA)_{1:4:1}$	452.11	596.47	56.25	225.27	0.255	1.28	0.758	1.082	1.0139	6.721
$(ChCl:EG:OA)_{1:4:1.5}$	458.59	607.42	57.00	222.09	0.251	1.26	0.755	1.133	1.0142	11.683
$(ChCl:EG:OA)_{1:4:2}$	464.14	616.92	57.65	219.37	0.246	1.23	0.752	1.179	1.0144	16.240
$(ChCl:EG:TA)_{1:4:0.5}$	464.94	605.70	55.08	242.25	0.265	1.35	0.768	1.035	1.1125	−6.970
$(ChCl:EG:TA)_{1:4:1}$	490.31	636.68	55.36	250.63	0.262	1.41	0.770	1.094	1.1129	−1.706
$(ChCl:EG:TA)_{1:4:1.5}$	511.48	662.69	55.58	257.21	0.26	1.44	0.771	1.143	1.1359	0.636
$(ChCl:EG:TA)_{1:4:2}$	529.63	684.90	55.72	262.85	0.257	1.46	0.773	1.185	1.1432	3.637
$(ChCl:EG:TA)_{1:4:3}$	559.12	720.87	55.83	272.01	0.253	1.49	0.775	1.252	1.1565	8.218
$(ChCl:EG:TA)_{1:4:4}$	582.06	748.73	55.85	279.14	0.250	1.51	0.777	1.303	1.1998	8.581
$(ChCl:Gly)_{1:4}$	526.96	666.40	52.32	294.41	0.278	1.64	0.790	1.017	1.012	0.455
$(ChCl:Gly:MA)_{1:4:0.5}$	530.03	674.43	52.61	289.24	0.271	1.58	0.785	1.061	1.0131	0.457
$(ChCl:Gly:MA)_{1:4:1}$	532.33	680.69	52.69	285.52	0.266	1.54	0.782	1.099	1.0135	4.693
$(ChCl:Gly:MA)_{1:4:1.5}$	534.40	686.49	52.83	282.1	0.261	1.49	0.778	1.134	1.0142	8.448
$(ChCl:Gly:MA)_{1:4:2}$	536.17	691.61	52.95	279.16	0.257	1.45	0.775	1.164	1.0146	11.774
$(ChCl:Gly:MA)_{1:4:3}$	539.05	700.21	53.15	274.40	0.250	1.39	0.770	1.217	1.0147	14.774
$(ChCl:Gly:MA)_{1:4:4}$	541.29	707.17	53.30	270.70	0.245	1.33	0.765	1.261	1.0149	19.984
$(ChCl:Gly:MA)_{1:4:5}$	543.08	712.90	53.43	267.73	0.241	1.30	0.761	1.298	1.015	24.274
$(ChCl:Gly:MA)_{1:4:6}$	544.54	717.70	53.53	265.31	0.238	1.27	0.759	1.329	1.0152	27.882
$(ChCl:Gly:MA)_{1:4:7}$	545.77	721.79	53.61	263.29	0.235	1.24	0.756	1.356	1.0154	30.937
$(ChCl:Gly:MA)_{1:4:8}$	546.80	725.30	53.68	261.58	0.232	1.21	0.753	1.380	1.0159	33.563
$(ChCl:Gly:MA)_{1:4:9}$	547.69	728.36	53.75	260.11	0.230	1.19	0.751	1.400	1.0169	35.803
$(ChCl:Gly:OA)_{1:4:0.5}$	527.98	672.31	53.45	284.10	0.271	1.59	0.785	1.065	1.0123	5.178
$(ChCl:Gly:OA)_{1:4:1}$	528.52	676.79	54.26	276.0	0.266	1.54	0.780	1.108	1.0129	9.411
$(ChCl:Gly:OA)_{1:4:1.5}$	529.12	681.13	55.04	268.92	0.261	1.50	0.777	1.148	1.0135	13.296
$(ChCl:Gly:OA)_{1:4:2}$	529.63	685.01	55.73	262.85	0.257	1.46	0.773	1.185	1.014	16.865
$(ChCl:Gly:TA)_{1:4:0.5}$	548.61	694.03	52.83	297.80	0.272	1.65	0.790467	1.076	1.1201	−3.981
$(ChCl:Gly:TA)_{1:4:1}$	566.73	716.74	53.04	301.37	0.268	1.65	0.790703	1.125	1.1234	0.139
$(ChCl:Gly:TA)_{1:4:1.5}$	582.02	736.10	53.26	304.044	0.265	1.67	0.790685	1.167	1.1456	1.883
$(ChCl:Gly:TA)_{1:4:2}$	595.13	752.70	53.43	306.34	0.261	1.66	0.790668	1.204	1.1579	3.947
$(ChCl:Gly:TA)_{1:4:3}$	616.44	779.67	53.67	310.06	0.257	1.66	0.790642	1.263	1.196	5.624
$(ChCl:Gly:TA)_{1:4:4}$	582.063	748.73	55.85	279.14	0.250	1.51	0.777396	1.303	1.196	8.926

4. Conclusion

A series of ternary deep eutectic solvents were designed and synthesized successfully. The FTIR analysis confirmed that hydrogen bonding is the main force responsible for the formation of deep eutectic solvents. The thermal stability of the ternary deep eutectic solvent was improved after the addition of carboxylic acids to ethaline and glyceline binary DES system. The physical properties such as density and viscosity of the binary DES system increased after the addition of the third component. While the surface tension of the system decreases resulting in the increase of void radius making it a suitable solvent as an extractant. The addition of the third component has no effect on the refractive of the system as clear homogenous mixture is formed. A Modified- Lyderson-joback and Lee-Kesler mixing rule was applied successfully for measuring the critical properties such as molecular weight (M), critical temperature (T_c), critical volume (V_c), ratio of normal boiling point to critical temperature (T_b/T_c) of the novel ternary deep eutectic solvent. Spensor and Danner correlation was successfully used to estimate the density of the synthesized TDES and compared with the experimental values. The %Δρ deviation was observed which increases with an increase in the molar ratio of the third component. The deviation varied from 0.2 % to 23 %. The above investigation will provide novel ternary deep eutectic solvent to be used as good extracting liquid in liquid extraction process.

CRediT authorship contribution statement

Mshari A. Alotaibi: Conceptualization, Data curation, Funding acquisition, Writing – original draft, Writing – review & editing. **Tabassum Malik:** Conceptualization, Data curation, Methodology, Writing – original draft, Writing – review & editing. **A. Naeem:**

Conceptualization, Supervision. **Amir Sada Khan:** Conceptualization, Supervision. **Israf Ud din:** Conceptualization, Data curation, Formal analysis. **Maizatul S. Shaharun:** Conceptualization, Formal analysis.

Declaration of competing interest

The authors declare that they have no known competing financial interests or personal relationships that could have appeared to influence the work reported in this paper.

Acknowledgement

The authors extend their appreciation to the Deputyship for Research & Innovation, Ministry of Education in Saudi Arabia for funding this research work through the project number IF2-PSAU-2022/01/22143.

References

[1] I.I. Alkhatib, D. Bahamon, F. Llovell, M.R. Abu-Zahra, L.F. Vega, Perspectives and guidelines on thermodynamic modelling of deep eutectic solvents, J. Mol. Liq. 298 (2020) 112183.
[2] R. Hayes, S. Imberti, G.G. Warr, R. Atkin, Effect of cation alkyl chain length and anion type on protic ionic liquid nanostructure, J. Phys. Chem. C 118 (25) (2014) 13998–14008.
[3] B. Villemejeanne, S. Legeai, E. Meux, S. Dourdain, H. Mendil-Jakani, E. Billy, Halide based ionic liquid mixture for a sustainable electrochemical recovery of precious metals, J. Environ. Chem. Eng. 10 (1) (2022) 107063.
[4] L. Manyoni, B. Kabane, G.G. Redhi, Deep eutectic solvent as a possible entrainer for industrial separation problems: pre-screening tool for solvent selection, Fluid Phase Equil. 553 (2022) 113266.
[5] F. Ghaffari, M.T. Zafarani-Moattar, H. Shekaari, Aqueous biphasic systems created with choline chloride-fructose natural deep eutectic solvents and polypropylene glycol 400 and usage of these systems for extraction of some commonly used drugs, Fluid Phase Equil. 555 (2022) 113348.
[6] F. Liu, L. Chen, K. Yin, T. Fan, Z. Yan, Sugars as hydrogen-bond donors tune the phase behavior in a novel liquid–liquid biphasic system formed by hydrophilic deep eutectic solvents and n-propanol, Fluid Phase Equil. 556 (2022) 113393.
[7] Q. Zhang, K.D.O. Vigier, S. Royer, F. Jerome, Deep eutectic solvents: syntheses, properties and applications, Chem. Soc. Rev. 41 (21) (2012) 7108–7146.
[8] C. Lopes, P. Velho, E.A. Macedo, Predicting the ionicity of ionic liquids in binary mixtures based on solubility data, Fluid Phase Equil. 567 (2023) 113717.
[9] A. Romero, A. Santos, J. Tojo, A. Rodríguez, Toxicity and biodegradability of imidazolium ionic liquids, J. Hazard Mater. 151 (1) (2008) 268–273.
[10] K.A. Omar, R. Sadeghi, Novel benzilic acid-based deep-eutectic-solvents: preparation and physicochemical properties determination, Fluid Phase Equil. 522 (2020) 112752.
[11] X. Wang, B. Liu, H. Yang, J. Tian, Properties of binary mixtures of a novel natural deep eutectic solvent (glycolic acid+ xylitol) and water at several temperatures, Fluid Phase Equil. 556 (2022) 113390.
[12] M. Jafari, S.Z. Shafaie, H. Abdollahi, A. Entezari-Zarandi, Green recycling of spent Li-ion batteries by deep eutectic solvents (DESs): leaching mechanism and effect of ternary DES, J. Environ. Chem. Eng. 10 (6) (2022) 109014.
[13] Y. Liao, S. Gong, G. Wang, T. Wu, X. Meng, Q. Huang, et al., A novel ternary deep eutectic solvent for efficient recovery of critical metals from spent lithium-ion batteries under mild conditions, J. Environ. Chem. Eng. 10 (6) (2022) 108627.
[14] F.O. Farias, F.H.B. Sosa, L. Igarashi-Mafra, J.A.P. Coutinho, M.R. Mafra, Study of the pseudo-ternary aqueous two-phase systems of deep eutectic solvent (choline chloride: sugars)+ K2HPO4+ water, Fluid Phase Equil. 448 (2017) 143–151.
[15] M.H. Chakrabarti, F.S. Mjalli, I.M. AlNashef, M.A. Hashim, M.A. Hussain, L. Bahadori, et al., Prospects of applying ionic liquids and deep eutectic solvents for renewable energy storage by means of redox flow batteries, Renew. Sustain. Energy Rev. 30 (2014) 254–270.
[16] M. Faraji, F. Noormohammadi, M. Adeli, Preparation of a ternary deep eutectic solvent as extraction solvent for dispersive liquid-liquid microextraction of nitrophenols in water samples, J. Environ. Chem. Eng. 8 (4) (2020) 103948.
[17] R. Yusof, E. Abdulmalek, K. Sirat, M.B.A. Rahman, Tetrabutylammonium bromide (TBABr)-Based deep eutectic solvents (DESs) and their physical properties, Molecules 19 (6) (2014) 8011–8026.
[18] H. Shirota, T. Mandai, H. Fukazawa, T. Kato, Comparison between dicationic and monocationic ionic liquids: liquid density, thermal properties, surface tension, and shear viscosity, J. Chem. Eng. Data 56 (5) (2011) 2453–2459.
[19] A.P. Abbott, A.Y. Al-Murshedi, O.A. Alshammari, R.C. Harris, J.H. Kareem, I.B. Qader, et al., Thermodynamics of phase transfer for polar molecules from alkanes to deep eutectic solvents, Fluid Phase Equil. 448 (2017) 99–104.
[20] C. Florindo, F.S. Oliveira, L.P.N. Rebelo, A.M. Fernandes, I.M. Marrucho, Insights into the synthesis and properties of deep eutectic solvents based on cholinium chloride and carboxylic acids, ACS Sustain. Chem. Eng. 2 (10) (2014) 2416–2425.
[21] T. Aissaoui, A. Im, Neoteric FT-IR investigation on the functional groups of phosphonium-based deep eutectic solvents, Pharm. Anal. Acta 6 (2015) 11.
[22] D.L. Pavia, G.M. Lampman, G.S. Kriz, J. Vyvyan, Introduction to Spectroscopy Cengage Learning, vol. 153, Ainara López Maestresalas, 2008.
[23] P. Larkin, Infrared and Raman Spectroscopy: Principles and Spectral Interpretation, Elsevier, 2017.
[24] A.P. Abbott, G. Capper, D.L. Davies, R.K. Rasheed, Ionic liquid analogues formed from hydrated metal salts, Eur. J. Chem. 10 (15) (2004) 3769–3774.
[25] N.L. Wang, X.Y. Zhang, P.H. Wang, Tartaric acid-assisted co-precipitation synthesis of Er3+-doped Lu2O3 nanopowders, Chin. J. Chem. 23 (11) (2012) 1299–1302.
[26] R.K. Banjare, M.K. Banjare, K. Behera, S. Pandey, K.K. Ghosh, Micellization behavior of conventional cationic surfactants within glycerol-based deep eutectic solvent, ACS Omega 5 (31) (2020) 19350–19362.
[27] G.M. Thorat, H.S. Jadhav, A. Roy, W.-J. Chung, J.G. Seo, Dual role of deep eutectic solvent as a solvent and template for the synthesis of octahedral cobalt vanadate for an oxygen evolution reaction, ACS Sustain. Chem. Eng. 6 (12) (2018) 16255–16266.
[28] S.L. Perkins, P. Painter, C.M. Colina, Experimental and computational studies of choline chloride-based deep eutectic solvents, J. Chem. Eng. Data 59 (11) (2014) 3652–3662.
[29] G. Li, C. Gui, R. Zhu, Z. Lei, Deep eutectic solvents for efficient capture of cyclohexane in volatile organic compound s: thermodynamic and molecular mechanism, AIChE J. 68 (3) (2022) e17535.
[30] H. Ghaedi, M. Ayoub, S. Sufian, B. Lal, Y. Uemura, Thermal stability and FT-IR analysis of Phosphonium-based deep eutectic solvents with different hydrogen bond donors, J. Mol. Liq. 242 (2017) 395–403.
[31] U. Saeed, A.L. Khan, M.A. Gilani, M.R. Bilad, A.U. Khan, Supported liquid membranes comprising of choline chloride based deep eutectic solvents for CO2 capture: influence of organic acids as hydrogen bond donor, J. Mol. Liq. 335 (2021) 116155.
[32] A. Lydersen, Estimation of critical properties of organic compounds, Univ Wisconsin Coll Eng, Eng Exp Stn Rep 3 (1955).
[33] K. Klincewicz, R. Reid, Estimation of critical properties with group contribution methods, AIChE J. 30 (1) (1984) 137–142.
[34] S. Labinov, J. Sand, An analytical method of predicting Lee-Kesler-Plöcker equation-of-state binary interaction coefficients, Int. J. Thermophys. 16 (1995) 1393–1411.

[35] J.O. Valderrama, B.F. Abu-Sharkh, Generalized rackett-type correlations to predict the density of saturated liquids and petroleum fractions, Fluid Phase Equil. 51 (1989) 87–100.
[36] C.F. Spencer, R.P. Danner, Improved equation for prediction of saturated liquid density, J. Chem. Eng. Data 17 (2) (1972) 236–241.
[37] N.R. Mirza, N.J. Nicholas, Y. Wu, S. Kentish, G.W. Stevens, Estimation of normal boiling temperatures, critical properties, and acentric factors of deep eutectic solvents, J. Chem. Eng. Data 60 (6) (2015) 1844–1854.